Bioorganic & Medicinal Chemistry Letters xxx (2018) xxx–xxx

Contents lists available at ScienceDirect

Bioorganic & Medicinal Chemistry Letters

journal homepage: www.elsevier.com/locate/bmcl

P3-P4 ureas and reverse carbamates as potent HCV NS3 protease inhibitors: Effective transposition of the P4 hydrogen bond donor

Brian L. Venables *, Ny Sin, Alan Xiangdong Wang, Li-Qiang Sun, Yong Tu, Dennis Hernandez, Amy Sheaffer, Min Lee, Cindy Dunaj, Guangzhi Zhai, Diana Barry, Jacques Friborg, Fei Yu, Jay Knipe, Jason Sandquist, Paul Falk, Dawn Parker, Andrew C. Good, Ramkumar Rajamani, Fiona McPhee, Nicholas A. Meanwell, Paul M. Scola

Bristol-Myers Squibb Research and Development, 5 Research Parkway, Wallingford, CT 06492, United States

ARTICLE INFO

Article history:
Received 31 December 2017
Revised 2 April 2018
Accepted 4 April 2018
Available online xxxx

Keywords:
HCV NS3
Inhibitors
Hepatitis C
Protease

ABSTRACT

A series of tripeptidic acylsulfonamide inhibitors of HCV NS3 protease were prepared that explored structure-activity relationships (SARs) at the P4 position, and their *in vitro* and *in vivo* properties were evaluated. Enhanced potency was observed in a series of P4 ureas; however, the PK profiles of these analogues were less than optimal. In an effort to overcome the PK shortcomings, modifications to the P3-P4 junction were made. This included a strategy in which one of the two urea N–H groups was either *N*-methylated or replaced with an oxygen atom. The former approach provided a series of regioisomeric *N*-methylated ureas while the latter gave rise to P4 reverse carbamates, both of which retained potent NS3 inhibitory properties while relying upon an alternative H-bond donor topology. Details of the SARs and PK profiles of these analogues are provided.

Approximately 185 million people worldwide are estimated to be infected with hepatitis C virus (HCV), a small, enveloped, positive strand RNA virus.[1,2] HCV is a major cause of chronic liver diseases such as cirrhosis and hepatocellular carcinoma.[3] Moreover, in the U.S., this virus has been the leading cause of liver transplant. The early standard of care, a combination of peg-interferon-α and ribavirin, was an important milestone in patient care. However, this approach ultimately proved only moderately effective in treating the disease and was associated with side effects, some of which were significant and prompted discontinuation of treatment.[4–6]

In an effort to provide interferon-free therapy, drug discovery efforts have been focused on the procurement of a direct-acting antiviral cocktail. Toward this end, small molecule discovery programs targeting the essential viral proteins NS3 protease, NS5A and NS5B have been studied extensively.[7] Our efforts in the NS3 protease arena led to the discovery of a potent series of acyl sulfonamide-based tripeptidic inhibitors.[8] BMS-605339 (**1**, Fig. 1) advanced to the clinic and demonstrated a significant antiviral response with a 1.8 $\log_{10}$ reduction in viral load after a single, 120 mg dose. However, further development of this compound was suspended due to a cardiovascular (CV) signal observed in patients receiving the drug. The CV liability associated with **1** was resolved in the discovery process that ultimately provided asunaprevir (**2**, Fig. 1).[9] The combination regimen of asunaprevir with the NS5A inhibitor daclatasvir (**3**, Fig. 1) was approved in Japan in July of 2014 for the treatment of patients with genotype (GT) 1b HCV infection.[10]

In the course of studies leading to the discovery of **2**, modifications at the P3-P4 interface of these tripeptide-based inhibitors were examined with the goal of improving potency while maintaining a PK profile similar to **1**.[11] In this report, we summarize those studies which led to the identification of a series of regioisomeric *N*-methylated ureas and P4 reverse carbamates that exhibited potent inhibition against the NS3 protease while relying upon an alternative H-bond donor topology to that in **1** and **2**. In addition, we summarize efforts to optimize the antiviral activity in this urea series while also exploring structural modifications of this functionality designed to optimize the PK properties.

Replacement of the *tert*-butyl carbamate endcap in **1** with a *tert*-butyl urea afforded **4** (Fig. 1), a compound with inhibitory potencies comparable to **1** against enzyme representing HCV NS3 GT 1a and against a HCV GT 1b replicon (Table 1). Urea **4** also demonstrated a 3-fold improvement in potency against NS3 protease enzymes representing GT 2b and GT 3a relative to carbamate **1**.

* Corresponding author.
E-mail address: brian.venables@bms.com (B.L. Venables).

https://doi.org/10.1016/j.bmcl.2018.04.009
0960-894X/

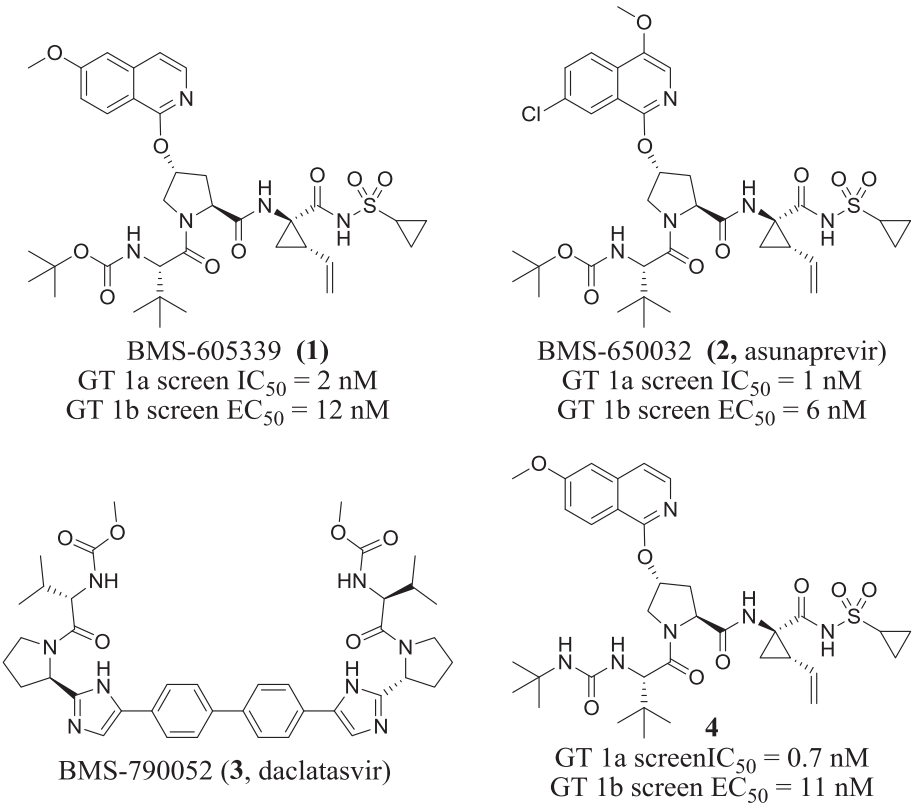

Fig. 1. BMS-605339 **(1)**, BMS-650032 asunaprevir (**2**), daclatasvir **(3)** and compound **4**.

Table 1
Structure, NS3 protease enzyme inhibition, HCV replicon cell-based inhibition, and solubility of various P3-P4 derivatives.

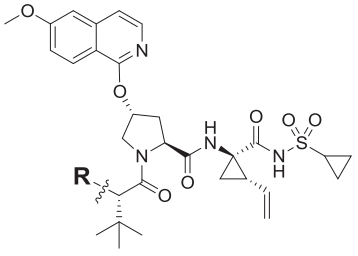

Compound	R	GT 1a[a] NS3/4a IC_{50} (nM)	GT 1b[b] NS3/4a EC50 (nM)	Solubility @ pH = 6.5 (mg/mL)	GT 2b[a] NS3/4a IC_{50} (nM)	GT 3a[a] NS3/4a IC_{50} (nM)	Rat Screen[c] Plasma AUC (ng h/mL)	Rat Screen[c] Liver Exposure @ 4 h (ng/g)
1	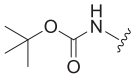	2.1	12	0.001	187	95	7423	64,708
4	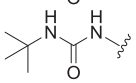	0.7	11	0.013	59	34	497	1110
7a	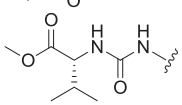	3.5	79		327	433		
7b	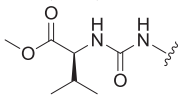	0.46	31		33	71		
8a	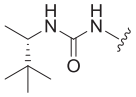	0.82	17		114	158		
8b	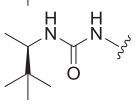	0.22	7.9		42	81		

Table 1 (*continued*)

Compound	R	GT 1a[a] NS3/4a IC_{50} (nM)	GT 1b[b] NS3/4a EC50 (nM)	Solubility @ pH = 6.5 (mg/mL)	GT 2b[a] NS3/4a IC_{50} (nM)	GT 3a[a] NS3/4a IC_{50} (nM)	Rat Screen[c] Plasma AUC (ng h/mL)	Rat Screen[c] Liver Exposure @ 4 h (ng/g)
9a	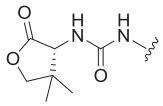	23	910					
9b	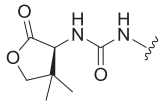	0.90	71					
10	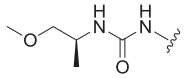	2.5	56	1.07	172	170		
11	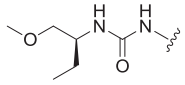	2	70	0.500	121	171		
12	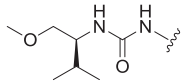	0.44	24	0.570	31	60		
13	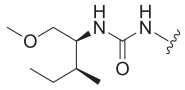	0.40	12	0.326	17	72		
14	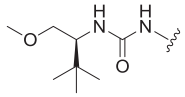	0.30	11	0.609	14	26	3275	838
15	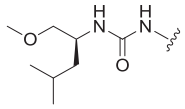	1.2	31	0.225	66	201		
16	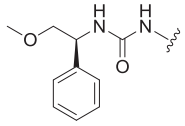	2.6	73	0.259	184	524		
17	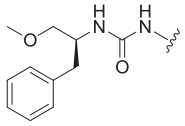	4.7	176	0.134	226	265		
18	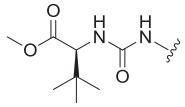	0.34	17	0.754	19	41		
19	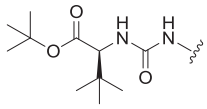	0.19	10	0.001	59	93	632	4849
20	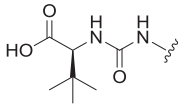	0.050	54	>1.16	9	11	91	0
21	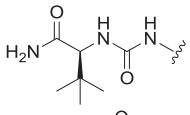	0.24	61	0.557	14	16		
22	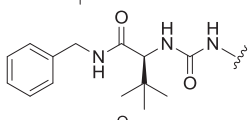	0.21	40	0.095	23	15		
23	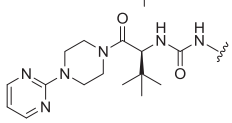	0.27	34	0.132	19	18	1631	87

[a] GT 1a = genotype 1a; GT 2b = genotype 2b; GT 3a = genotype 3a; HCV NS3 enzyme inhibitory activity was assessed according to the conditions described in Ref 13.
[b] GT 1b = genotype 1b; HCV replicon activity was assessed in the presence of 10% fetal bovine serum (FBS) according to the conditions described in Ref 13.
[c] Intraduodenal (ID) single dose, 15 mg/kg, $n = 2$, endpoint = 4 h using conditions described in Ref. 9a.

Please cite this article in press as: Venables B.L., et al. Bioorg. Med. Chem. Lett. (2018), https://doi.org/10.1016/j.bmcl.2018.04.009

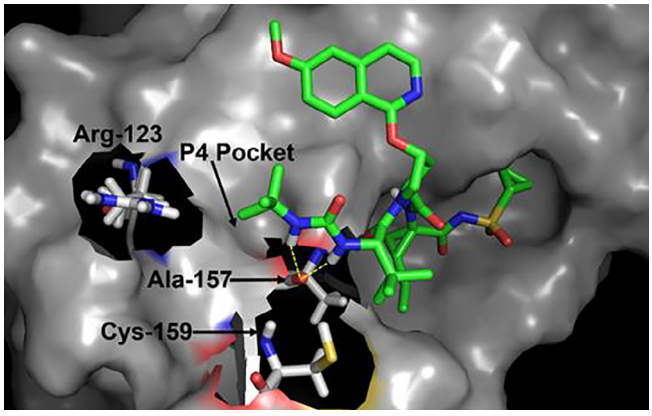

Fig. 2. Compound **4** modeled into the HCV NS3/4A protease GT1a binding site.

Computational modeling of **4** bound to a NS3/4A protease complex suggested that the urea motif of ligand **4** could participate in a bidentate hydrogen-bonding interaction with the backbone carbonyl of Ala-157, as depicted in Fig. 2.[12] Additionally, **4** demonstrated a 10-fold improvement in aqueous solubility relative to its carbamate counterpart **1**.

Based on its promising *in vitro* antiviral activity, the pharmacokinetic (PK) profile of **4** in the rat was examined. This compound was administrated *via* intraduodenal dosing and exposure levels in the plasma and liver were measured over a 4 h period. The concentration of **4** in both plasma and liver was found to be significantly lower than the levels observed after dosing **1** under the same protocol (Table 2). Despite the inferior PK profile of **4** compared to **1**, the exploration of P4 urea caps remained of interest given the enhanced potency toward NS3 protease enzymes representing GT 1a, GT 2b and GT 3a.

Table 2
Transpositioning of the P3-P4 hydrogen-bond donor.

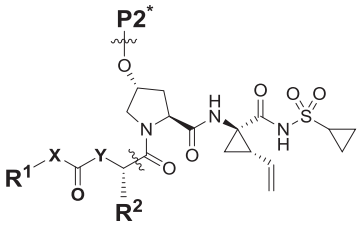

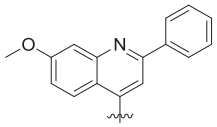

P2* #1

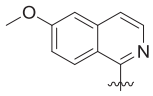

P2* #2

Compound	P2*	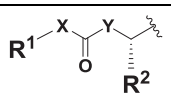	GT1a[a] NS3/4a IC50 (nM)	GT1b[b] NS3/4a EC50 (nM)	GT2b[a] NS3/4a IC50 (nM)	GT3a[a] NS3/4a IC50 (nM)	Rat Screen[c] Plasma AUC (ng h/mL)	Rat Screen[c] Liver Exposure @ 4 h (ng/g)
24	1	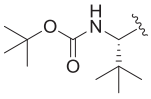	4.5	6.0	18	18	61	7850
25	1	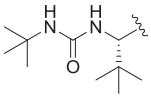	4.6	10	7.0	7.4	17	72
26	1	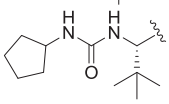	8.0	9.2	3.2	16		
27	1	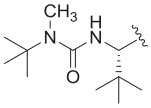	2.3	100	8.7	17	32	2602
28	1	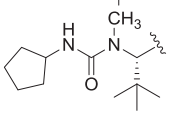	945	ND[d]				
29	1	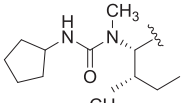	35	66			ND[d]	1243
30	1	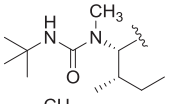	2.8	81			16	1776
31	2	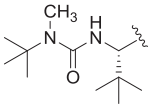	10	243				

Table 2 (*continued*)

Compound	P2*	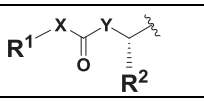	GT1a[a] NS3/4a IC50 (nM)	GT1b[b] NS3/4a EC50 (nM)	GT2b[a] NS3/4a IC50 (nM)	GT3a[a] NS3/4a IC50 (nM)	Rat Screen[c] Plasma AUC (ng h/mL)	Rat Screen[c] Liver Exposure @ 4 h (ng/g)
32	2	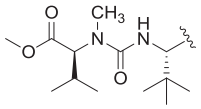	1.7	129				
33	1	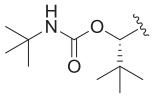	13	42			82	3772
34	1	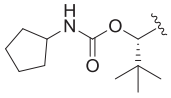	11	30	277	843	95	3431
35	1	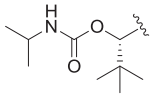	12	85			ND[d]	430

[a] GT 1a = genotype 1a; GT 2b = genotype 2b; GT 3a = genotype 3a; HCV NS3 enzyme inhibitory activity was assessed according to the conditions described in Ref. 13.
[b] GT 1b = genotype 1b; HCV replicon activity was assessed in the presence of 10% fetal bovine serum (FBS) according to the conditions described in Ref. 13.
[c] Intraduodenal (ID) single dose, 15 mg/kg, $n = 2$, endpoint = 4 h using conditions described in Ref. 9a.
[d] ND = not detected.

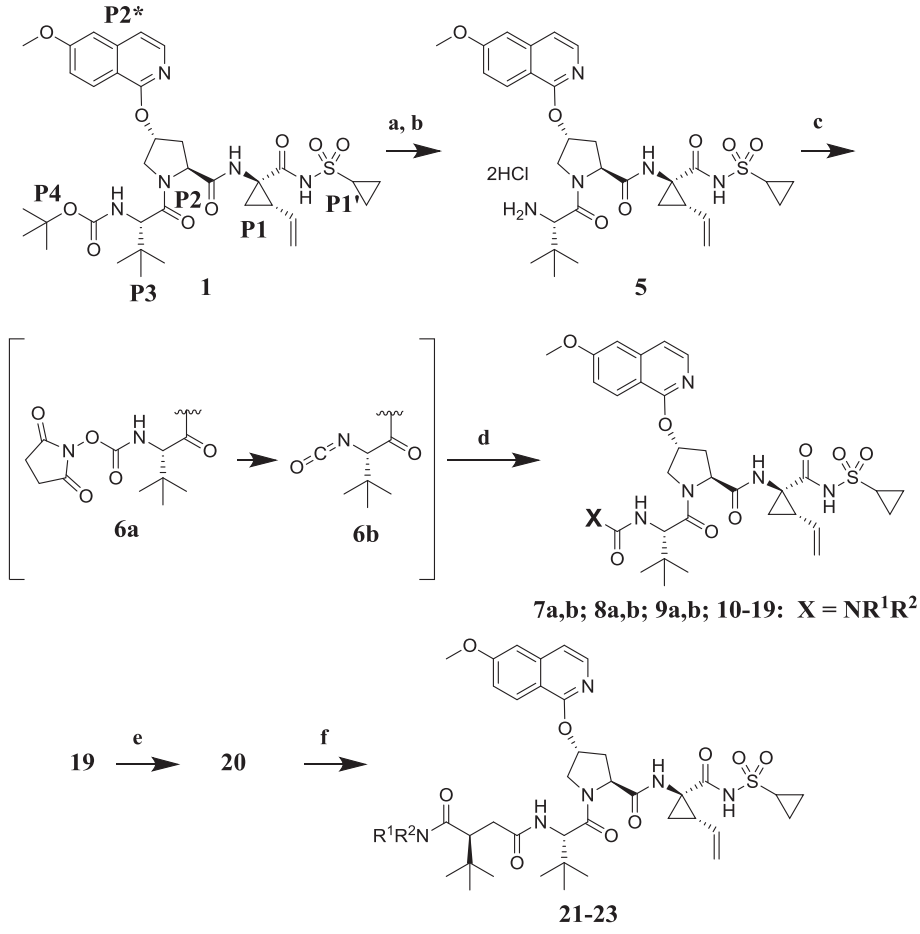

Fig. 3. Synthesis of P3-P4 ureas **7**–**19** and P4-P5 amides **21**–**23**. Reagents and conditions: a) 50% TFA in CH_2Cl_2, RT, quantitative; b) 1 M HCl in Et_2O, RT, 88%; c) *N,N'*-disuccinimidyl carbonate, DIPEA, THF, 70 °C, 30 min; d) R^1R^2NH, THF, RT, 18 h, 20–82% yield from **5**; e) 50% TFA in DCM, RT, 96% yield; f) R^1R^2NH, HATU, *N*-methylmorpholine, DCM, RT, 18 h, 39–81% yield.

A general synthesis of P3-P4 ureas was devised and is depicted in Fig. 3. *N*-Boc deprotection of **1** with TFA in CH_2Cl_2 followed by conversion to the hydrochloride salt provided amine **5** as a powder isolable by simple filtration. Treatment of **5** with *N,N'*-disuccinimidyl carbonate afforded a mixture of the succinimidyl carbonate **6a** and isocyanate **6b**. The crude mixture was treated directly with

excess amine to provide the desired ureas **7**–**19** in good overall yield. A series of P4-P5 amides was prepared *via* hydrolysis of the *tert*-butyl ester in **19** followed by subsequent HATU-mediated coupling of the resultant acid **20** with various amines to give the series of amides **21**–**23**.

All compounds were tested for enzyme inhibitory activity toward a homogeneous full-length HCV GT 1a NS3/4A protease complex with the more active molecules additionally tested against NS3/4A complexes representing GT 2b and 3a proteases.[9b,13] Activity was assessed using a fluorescence resonance energy transfer (FRET) assay and the 50% inhibitory concentration (IC_{50}) values were determined as previously described.[14,15] The concentration required for half maximal inhibition of virus replication in a GT 1b (Con1) replicon was determined and the data reported as EC_{50} values. Construction of the replicon cell line has been described previously.[16] Aqueous solubility was determined in phosphate buffer solution at pH = 6.5. These data are compiled in Tables 1 and 2.

In the course of preparing a series of P3-P4 urea analogs, it was discovered that urea **7b**, which contains L-valine methyl ester as the P4 endcap (Table 1), offered an ~8-fold potency advantage over the corresponding D-valine methyl ester **7a**. This observed stereochemical preference at P4 was recapitulated with the diastereomeric pair of ureas **8a**/**8b** and **9a**/**9b** where the L-isomer showed a several-fold increase in potency relative to the D-isomer. Computational modeling suggested that the enhancement in activity observed for compounds in the L-stereochemical series was due to a beneficial hydrophobic surface interaction between enzyme and inhibitor at the lipophilic P4 pocket of the protease, as previously reported.[11b,17]

In an attempt to further optimize interactions in the lipophilic P4 pocket, we next prepared compounds **10**–**17** (Table 1) which possessed the preferred stereochemistry at P4, but with R-groups of varying size and shape. In addition to providing important structural information for maximizing potency, these compounds were engineered with the goal of improving PK. We reasoned that the terminal methyl ether oxygen of **10**–**17** might form an intramolecular hydrogen-bond with the urea moiety, effectively presenting the end of the molecule as a pseudo 5-membered ring, and thereby masking a portion of the urea polarity and potentially improving permeability.[18,19] Compound **14** proved to be the most active in this series, with anti-NS3 protease activity in the GT 1a and GT 3a biochemical assays ~3-fold more potent than that observed for compound **4**. SAR trends in this series were sensitive to steric bulk, with *in vitro* anti-NS3 protease activities generally deteriorating as R became either smaller (compounds **10**–**13**) or larger (compounds **15**–**17**) than the *tert*-butyl moiety of compound **14**. With respect to PK properties, a 6-fold increase in plasma AUC was observed for compound **14** compared to urea **4** while liver concentrations were found to be similar for these analogues. Interestingly, this PK improvement was coincidental with a ~50-fold increase in aqueous solubility of **14** when compared to **4**. Given these data, we speculated that the terminal P4 ether moiety in **14** may be driving solubility by providing a more polar terminus compared to **4**. This enhanced solubility may also explain the increase in absorption for **14** compared to **4**. However, the potential for the terminal methyl ether in **14** to facilitate the desolvation of the P4 urea through the formation of an intramolecular hydrogen-bond that obscures the polarity of the urea should also be considered as a source of improved absorption of **14**. Although the PK result for **14** marked progress within the urea series, the exposure observed for this compound was inferior to that of carbamate **1** and, hence, attention was focused on replacement of the P4 methyl ether end cap in an effort to further modulate anti-NS3 protease activity and improve PK.

The P4 cap functionality explored in this part of the survey included esters, amides and acidic groups, as exemplified by compounds **18**–**23** in Table 1. It should be noted that the P4 *tert*-butyl group present in **14** was a fixed structural element in this series since the SAR suggested optimal complementarity between this lipophilic substituent and the complementary pocket of the enzyme. In the event, esters **19** and **20** and amides **21**–**23** were found to exert similar anti-NS3 protease activity in the biochemical assay although they did not provide a significant improvement in potency compared to **14**. This observation suggested that the immediate P4 caps were not interfacing with the enzyme surface but were instead solvent-exposed. The PK profile of compounds **19** and **20** provided no significant improvement over the simpler congener **14**. Interestingly, compound **20**, which bears a carboxylic acid as a P4 cap, demonstrated a significant improvement in potency in the biochemical assays across NS3 proteases representing GTs 1–3. Most notable was the IC_{50} value toward the GT 1a enzyme which, at 50 pM, was 6-fold more potent than compound **14**. Docking studies suggested that the enhanced potency of **20** could be attributed to hydrogen-bonding interactions between the terminal carboxylate of **20** and both Arg-123 as well as the backbone NH of Cys-159 (Fig. 4). While this level of activity in the biochemical assay was significant, the PK profile of **20** was less than optimal and hence this compound was not progressed.

As noted above, a model of **4**, bound to the NS3/4a protease enzyme complex suggested that the P4 urea moiety could potentially bind to the carbonyl moiety of Ala-157 in a bidentate fashion (Fig. 2), while P4 carbamates such as **1** interface with the enzyme through a single H-bond interaction.[12,8] Given the potency of carbamate **1**, we sought to examine the idea that acceptable inhibition of the NS3 protease may be achievable with substrates possessing a single H-bond donor projected distal rather than proximal to the P3 moiety. To this end, both *N*-methylated urea derivatives as well as reverse carbamates were prepared in effort to explore this concept and the results are summarized in Table 2. Synthetic schema for the preparations of these compounds can be found in the Supplemental Material.

A series of P3-P4 ureas were explored first and their anti-NS3 protease activity, antiviral properties in a HCV replicon cell-based assay and PK profiles examined. Installation of a methyl group on the P4 side nitrogen atom of the urea yielded **27**, a molecule which retained intrinsic potency against the GT 1a NS3 protease but exhibited reduced potency in the GT 1b replicon cell-based assay when compared to the parent urea analogue **25**. Transposition of the methyl group to the P3 side of the urea provided **28**, a compound with poor potency in the biochemical assay. While this result appeared discouraging with respect to the hypothesis under examination, a model of **28** bound to the NS3/4a protease complex

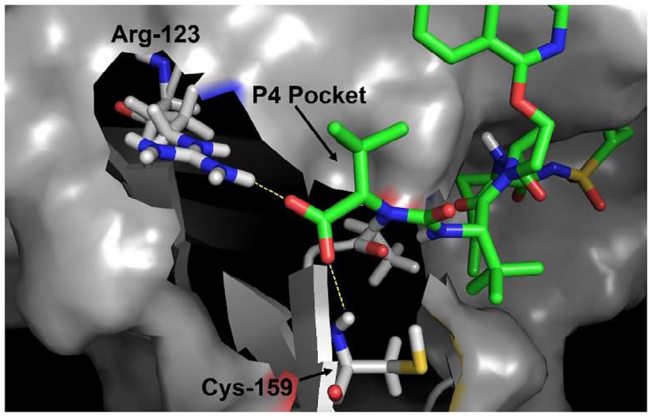

Fig. 4. Compound **19** modeled into the GT 1a HCV NS3/4A protease complex binding site.

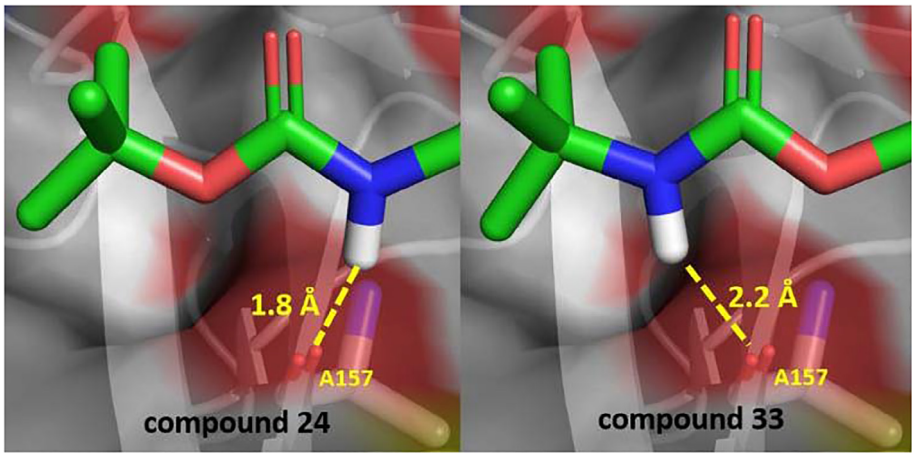

Fig. 5. The P4 termini of compounds **24** and **33** modeled into the HCV GT 1a NS3/4A protease complex binding site.

suggested that steric repulsion between the urea methyl substituent and the P3 *tert*-butyl moiety may result in a local conformation in which hydrogen-bonding between the remaining urea N–H and the carbonyl of Ala-157 was unfavorable. In order to probe relief of this potential source of steric strain in **28**, replacement of the P3 *tert*-butyl with the corresponding *sec*-butyl group was examined. This subtle but important structural modification restored inhibitory properties against the enzyme, as exemplified by compounds **29** and **30**. Compounds **27**, **29** and **30** offered comparable performance in the rat PK screen but each demonstrated significantly enhanced (17 to 36-fold) liver levels when compared to the parent urea **25**. However, plasma levels for these compounds remained relatively low and this series was not progressed.

In an effort to further the observation that the hydrogen-bond donor could reside on either side of the P4 carbonyl oxygen atom, we next considered a series of reverse carbamates in the context of **33**–**35** since the oxygen atom would present a sterically relatively undemanding element at this site of the pharmacophore. Modeling of carbamate **24** and reverse carbamate **33** with the NS3/4a protease complex illustrated the similarity of the hydrogen-bond distances between the carbamoyl NH of the two compounds and the backbone carbonyl of Ala-157 (Fig. 5). The observed improvement in potency against the NS3 protease with reverse carbamates **33**–**35** was notable, just 3-fold less than the parent carbamate **24**. However, the PK profile of compounds **33**–**35** after ID dosing was similar to the parent series and hence reverse carbamates appeared to offer no advantage over the parent series represented by **24**. It should be noted that the use of a reverse carbamate functionality at the P3-P4 position of inhibitors of serine protease has found somewhat limited application.[20] However, the activity observed with this functionality in the current series suggests that reverse carbamates may be a viable replacement for *N*-terminal amide or carbamate capping groups.

In summary, we have described the design of a series of P3-P4 urea-linked compounds that provided significant intrinsic antiviral potency as well as aqueous solubility advantages over P3-P4 carbamate-linked tripeptide HCV NS3 protease inhibitors. The lipophilic P4 structural component of these inhibitors was adjusted to provide for optimal potency. The concept of hydrogen-bond donor transposition at the P3-P4 junction was successfully demonstrated with both *N*-methylated ureas and reverse carbamates. Despite several advantages discovered with the P3-P4 ureas, these derivatives were characterized by permeability and exposure shortcomings, presumably due to the inherent polarity of the urea motif itself. A strategy to overcome these shortcomings was implemented with moderate success but, ultimately, the PK profiles of the P3-P4 urea compounds did not yield the targeted PK parameters, leading to this series being dropped from further consideration.

A. Supplementary data

Supplementary data associated with this article can be found, in the online version, at https://doi.org/10.1016/j.bmcl.2018.04.009.

References

1. Mohd HK, Groeger J, Flaxman AD, Wiersma ST. *Hepatology*. 2013;57:1333–1342.
2. Messina JP, Humphreys I, Flaxman A, et al. *Hepatology*. 2015;61:77–87.
3. Simonetti RG, Cammá C, Fiorello F, et al. *Ann Intern Med*. 1992;116:97–102.
4. Sulkowski MS, Cooper C, Hunyady B, et al. Nat Rev. *Gastroenterol Hepatol*. 2011;8:212–223.
5. Ogawa E, Furusyo N, Kajiwara E, et al. The Kyushu University Liver Disease Study [KULDS] Group. *J Gastroenterol Hepatol*. 2012;27:1233–1240.
6. Fried MW. *Hepatology*. 2002;36(Suppl. 1):S237–S244.
7. Appel N, Schaller T, Penin F, Bartenschlager R. *J Biol Chem*. 2006;281:9833–9836.
8. Scola PM, Wang AX, Good AC, et al. *J Med Chem*. 2014;57:1708–1729.
9. (a) Scola PM, Sun L-Q, Wang AX, et al. *J Med Chem*. 2014;57:1730–1752;
(b) McPhee F, Sheaffer AK, Friborg J, et al. *Antimicrob Agents Chemother*. 2012;56:5387–5396.
10. (a) Gao M, Nettles RE, Belema M, et al. *Nature*. 2010;465:96–100;
(b) Belema M, Nguyen VN, Bachand C, et al. *J Med Chem*. 2014;57:2013–2032;
(c) Poole RM. *Drugs*. 2014;74:1559–1571;
(d) Kumada H, Suzuki Y, Ikeda K, et al. *Hepatology*. 2014;59:2083–2091.
11. (a) Campbell JA, Good A. *PCT Int Appl WO*. 2002. 2002060926;
(b) Wang XA, Sun L-Q, Sit S-Y, et al. *PCT Int Appl WO*. 2003. 2003099274;
(c) Sin N, Good A, Venables B, Scola P, Meanwell N. *PCT Int Appl WO*. 2006. 2006086381.
12. Slater MJ, Amphlett EM, Andrews DM, et al. *Org Lett*. 2003;5:4627–4630.
13. Sheaffer AK, Lee MS, Hernandez D, et al. *Antivir Ther*. 2011;16:705–718.
14. Taliani M, Bianchi E, Narjes F, et al. *Anal Biochem*. 1996;240:60–67.
15. Drexler D, Barlow DJ, Falk P, et al. *Anal Bioanal Chem*. 2006;384:1145–1154.
16. Fridell RA, Qiu D, Wang C, Valera L, Gao M. *Antimicrob Agents Chemother*. 2010;54:3641–3650.
17. (a) Bogen SL, Pan W, Ruan S, et al. *PCT Int Appl WO*. 2005. 2005085275;
(b) Bogen SL, Pan W, Ruan S, et al. *J Med Chem*. 2009;52:3679–3688.
18. Lipinski CA, Lombardo F, Dominy BW, Feeney PJ. *Adv Drug Deliv Rev*. 1997;23:3–25.
19. (a) Gao H, Su P, Shi Y, et al. *Eur J Med Chem*. 2015;90:232–240;
(b) Furet P, Caravatti G, Guagnano V, Lang M, Meyer T, Schoepfer J. *Bioorg Med Chem Lett*. 2008;18:897–900;
(c) Sasaki S, Cho N, Nara Y, et al. *J Med Chem*. 2003;46:113–124;
(d) Ashwood VA, Field MJ, Horwell DC, et al. *J Med Chem*. 2001;44:2276–2285.
20. (a) Bailey MD, Bordeleau J, Garneau M, et al. *Bioorg Med Chem Lett*. 2013;23:4447–4452;
(b) Duan M, Kazmierski W, Crosby R, et al. *Bioorg Med Chem Lett*. 2012;22:2993–2996;
(c) Llinás-Brunet M, Bailey MD, Ghiro E, et al. *J Med Chem*. 2004;47:6584–6594;
(d) Saksena AK, Girijavallabhan VM, Lovey RG, et al. *PCT Int Appl WO*. 2003. 2003062265;
(e) Ohshima M, Iwase N, Sugiyama S, et al. *Eur Pat Appl EP*. 1995. 669317.